GCOM-C/SGLI Land Atmospheric Correction Algorithm

Hiroshi Murakami,
JAXA/EORC
Oct. 2018 (v1.000)

1 Overview of Algorithm

1.1 Definition of GCOM-C atmospheric corrected land surface reflectance (RSRF) product

- Surface reflectance of solid or liquid structures on the ground which includes canopy, snow, and water. Light scattering and absorption of atmospheric molecules and aerosol particles are corrected from clear sky top of atmosphere (TOA) reflectance.
- Directional dependency is not corrected for the snapshot (one-day) product, and corrected for the 8-day and monthly products.
- Slope effect correction, which normalizes solar irradiance change due to the land-surface slope, will be investigated in the post-launch evaluation.

1.2 Development strategy (discussed in the atmospheric correction workshop in Sep. 2012)

- The algorithm is mainly developed by JAXA/EORC through integration of knowledge about the atmosphere (aerosol scattering and absorption, and radiative transfer modeling), the land surface (spectral reflectance and bidirectional reflectance), and cloud (and snow cover) area detection in collaboration with PI groups.
- The algorithm considers consistency (e.g., candidate aerosol model and BRDF) with downstream products (land and atmosphere products) and sensor calibration characteristics including vicarious calibration by using other satellite sensors and in-situ observation, and calibration corrections.
- In-situ validation data (BRDF, solar irradiance, and aerosols) will be obtained by land-PIs (Honda, Chiba Univ., Nasahara, Tsukuba Univ., and so on). Atmospheric parameters will be obtained simultaneously as much as possible in collaboration with the atmosphere PIs.

1.3 Function and characteristics

- Output land surface reflectance by subtracting atmospheric molecules and aerosols from TOA radiance (reflectance) in the daytime clear sky areas.
- Reflectance is one at the satellite-solar geometric condition by consideration of land-surface BRDF by using multiple-day's data.

1.4 Interface in the GCOM-C processing flow

- Multiple day (32 days; the day number will be evaluated after the launch) precise geometric corrected tile-mapped TOA radiance (reflectance) data (LTOAQ) is used as the input.
- Dynamic look-up table (LUT) is used to use previous day's BRDF estimation for the aerosol correction.
- Output surface reflectance data (RSRF) is averaged for 8-day and monthly in the level-3 processing.

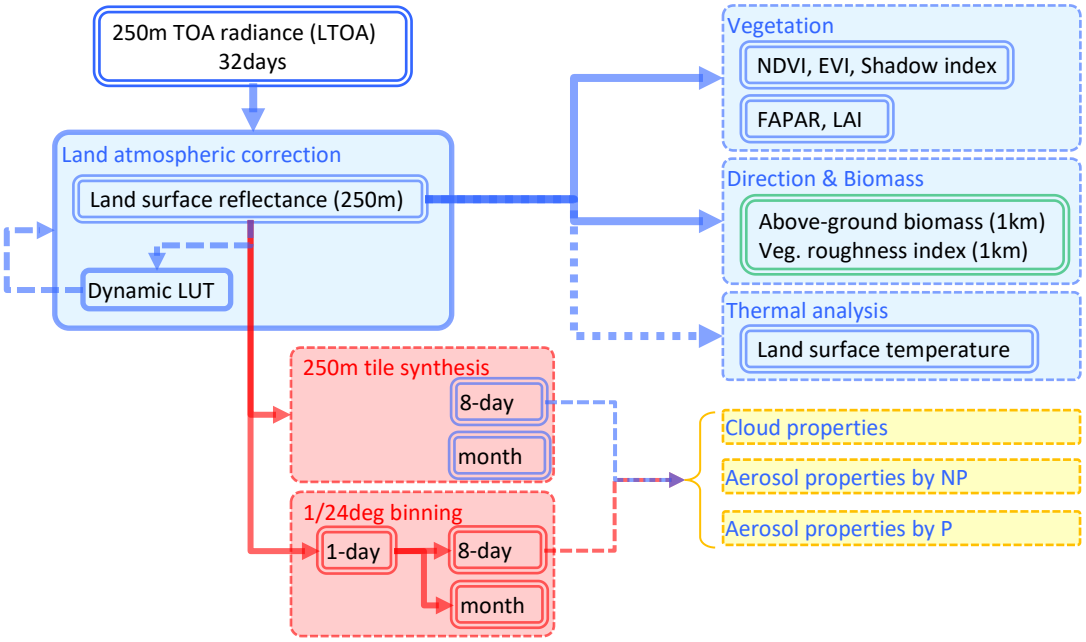

Fig. 1 Operation flow around the GCOM-C Land Atmospheric Correction

1.5 New development

- The land atmospheric correction is the new function from ADEOS-2/GLI in which aerosol was not corrected. This BRDF estimation scheme using the multiple day data has been developed by several studies by MODIS (Lyapustin et al., 2012) and higher-resolution sensors (Hajj et al., 2008, Hagolle et al., 2008), however it is not usual being the standard product because of estimation instability and long processing time.

1.6 Development history

- 2012/9: development strategy was discussed in the atmospheric correction workshop
- 2015/1/13：Deriver the first version code
- 2015/07/20: bug fix in lut_d/RSRF/*BRDFQ output and observation time handling
- 2015/09/03: bug fix in dataset name: Sensor_***_TI -> Sensor_***_IR
- 2016/01/29 (v005): change NG to Poor when n_in==0
- 2017/01/31 (v006): revision of the multi-day estimation module, and reduce the processing time, including correction of center-wavelength shift and slope effect

2 SGLI Land Atmospheric Correction Algorithm

2.1 Algorithm flow

- Input precise geometric corrected TOA reflectance data (LTOA) of 32 (variable) days. Both 250-m LTOA (LTOAQ) and 1-km LTOA (LTOAK) can be inputted (LTOAK input is not for the standard processing)
- Previous day's BRDF LUT (dynamic LUT) is inputted, and current day's BRDF LUT is outputted.

- Current day land surface reflectance (RSRF) is produced by the current day LTOA and current day BRDF LUT.
- The outputted RSRF is averaged for 8-day and monthly in the level-3 processing.
- The 8-day data is used for the atmospheric product processing

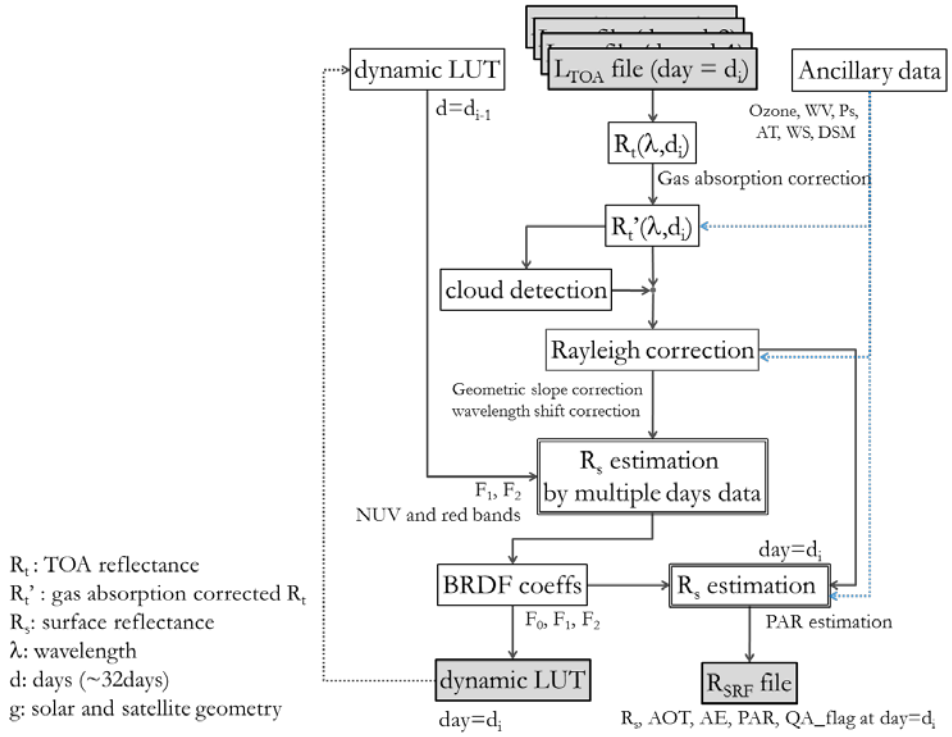

Figure 2 Overall flow of SGLI land atmospheric correction

2.2 Radiance to reflectance

TOA radiance L_{TOA} is converted to TOA reflectance ρ_{TOA} for each SGLI channel (λ)

$$\rho_{TOA}(\lambda) = \pi L_{TOA}(\lambda)\, d^2 / (F_0(\lambda) \cos(\theta_0))$$

where d is distance between the sun to the earth (1: 1AU), $F_0(\lambda)$ is SGLI-channel weighted solar irradiance (calculated by using Thuillier 2003), θ_0 is solar zenith angle.

Table 1 SGLI-band weighted center wavelength (λ_c) and solar irradiance (F_0)

band	λ_c (nm)	F_0 ($Wm^{-2}\mu m^{-1}$)	Min λ_c (nm)	F_0 ($Wm^{-2}\mu m^{-1}$)	Max λ_c (nm)	F_0 ($Wm^{-2}\mu m^{-1}$)
VN01	380.03	1092.14	379.80	1093.97	380.24	1090.67
VN02	412.51	1712.15	412.11	1710.45	412.68	1712.86
VN03	443.24	1898.32	442.96	1891.31	443.57	1906.81
VN04	489.85	1938.46	489.60	1937.76	490.39	1941.65
VN05	529.64	1850.96	529.47	1850.33	530.09	1852.37
VN06	566.15	1797.13	565.76	1797.75	566.56	1796.60
VN07	672.00	1502.55	671.73	1503.26	672.61	1500.80
VN08	672.10	1502.30	671.89	1502.87	672.67	1500.65
VN09	763.07	1245.45	762.35	1247.82	763.58	1243.79
VN10	866.76	956.34	866.11	955.99	867.48	956.52
VN11	867.12	956.62	866.40	956.29	867.90	956.71

PL01	671.89	1503.59	671.89	1503.60	673.10	1499.84
PL02	866.18	956.92	865.85	956.68	866.63	957.13
SW01	1054.99	646.54	NA	NA	NA	NA
SW02	1385.35	361.24	NA	NA	NA	NA
SW03	1634.51	237.58	NA	NA	NA	NA
SW04	2209.48	84.25	NA	NA	NA	NA
TI01	10792.98	0.00	NA	NA	NA	NA
TI02	11956.28	0.00	NA	NA	NA	NA

2.3 Gas absorption correction

Absorption coefficients of H_2O, O_3, and O_2 are calculated by PSTAR by the following equation.

$$\rho_{TOA}(\lambda)' = \rho_{TOA}(\lambda) / (t_g(\lambda)^{am})$$

$$t_g(\lambda) = exp\{ -(k_{oz0}(\lambda) + k_{oz1}(\lambda) \times (oz - oz_0)^{\alpha}) \times (oz - oz_0)$$
$$- (k_{wv0}(\lambda) + k_{wv1}(\lambda) \times (wv - wv_0)^{\alpha}) \times (wv - wv_0)$$
$$- (k_{ox0}(\lambda) + k_{ox1}(\lambda) \times (P - P_0)^{\alpha}) \times (P - P_0) \}$$

$$am = 1/\cos(\theta) + 1/\cos(\theta_0)$$

oz, wv, and P are column ozone (DU), column water vapor (mm), and relative surface pressure (1.0: 1013.25hPa). oz_0=343.79 DU, wv_0=14.186 mm, P_0=1013.25 hPa. θ is satellite zenith angle.

Table 2 Gas absorption coefficients of SGLI channels

gas	***Channel***	***λc min***			***λc max***		
		0	***1***	***a***	***0***	***1***	***a***
k_{wv}	***VN01***	1.5445E-06	0.0000E+00	0.00	1.48620E-06	0.00000E+00	0.00
	VN02	9.4948E-07	0.0000E+00	0.00	1.00540E-06	0.00000E+00	0.00
	VN03	3.1314E-05	0.0000E+00	0.00	3.20730E-05	0.00000E+00	0.00
	VN04	1.0517E-05	0.0000E+00	0.00	1.02670E-05	0.00000E+00	0.00
	VN05	1.6059E-05	0.0000E+00	0.00	1.79770E-05	0.00000E+00	0.00
	VN06	1.1847E-04	0.0000E+00	0.00	1.25530E-04	0.00000E+00	0.00
	VN07	5.9118E-05	0.0000E+00	0.00	5.21940E-05	0.00000E+00	0.00
	VN08	5.7061E-05	0.0000E+00	0.00	5.15330E-05	0.00000E+00	0.00
	VN09	2.1217E-06	0.0000E+00	0.00	1.39310E-06	0.00000E+00	0.00
	VN10	8.8784E-05	0.0000E+00	0.00	7.31440E-05	0.00000E+00	0.00
	VN11	8.4187E-05	0.0000E+00	0.00	6.97610E-05	0.00000E+00	0.00
	PL01	4.7346E-05	0.0000E+00	0.00	4.21620E-05	0.00000E+00	0.00
	PL02	8.3032E-05	0.0000E+00	0.00	7.26590E-05	0.00000E+00	0.00
	SW01	4.0931E-05	0.0000E+00	0.00			
	SW02	-2.5585E-01	1.4719E+00	-0.32			
	SW03	4.3975E-03	-2.8813E-03	0.06			
	SW04	1.7986E-02	-1.1061E-02	0.08			
k_{ox} ***(O2)***	***VN01***	1.6224E-03	0.0000E+00	0.00	1.62430E-03	0.00000E+00	0.00
	VN02	4.0746E-05	0.0000E+00	0.00	4.28740E-05	0.00000E+00	0.00
	VN03	4.5989E-04	0.0000E+00	0.00	4.83160E-04	0.00000E+00	0.00
	VN04	2.1982E-04	0.0000E+00	0.00	1.77910E-04	0.00000E+00	0.00
	VN05	1.1559E-03	0.0000E+00	0.00	1.16790E-03	0.00000E+00	0.00
	VN06	5.3377E-03	0.0000E+00	0.00	5.81480E-03	0.00000E+00	0.00
	VN07	1.1843E-03	0.0000E+00	0.00	1.72480E-03	0.00000E+00	0.00
	VN08	1.2444E-03	0.0000E+00	0.00	1.73980E-03	0.00000E+00	0.00
	VN09	3.0435E-02	2.8313E-01	-0.60	3.13240E-02	2.85120E-01	-0.60
	VN10	4.3529E-05	0.0000E+00	0.00	4.53640E-05	0.00000E+00	0.00
	VN11	4.3813E-05	0.0000E+00	0.00	4.74650E-05	0.00000E+00	0.00
	PL01	1.3550E-03	0.0000E+00	0.00	2.22670E-03	0.00000E+00	0.00
	PL02	4.2436E-05	0.0000E+00	0.00	4.23090E-05	0.00000E+00	0.00
	SW01	8.5098E-03	0.0000E+00	0.00			
	SW02	4.0890E-04	0.0000E+00	0.00			
	SW03	4.9989E-07	0.0000E+00	0.00			

	SW04	6.8205E-08	0.0000E+00	0.00			
k_{oz}	***VN01***	9.0074E-09	0.0000E+00	0.00	7.68290E-09	0.00000E+00	0.00
	VN02	2.4232E-07	0.0000E+00	0.00	2.59410E-07	0.00000E+00	0.00
	VN03	2.9846E-06	0.0000E+00	0.00	3.06890E-06	0.00000E+00	0.00
	VN04	2.0569E-05	0.0000E+00	0.00	2.08290E-05	0.00000E+00	0.00
	VN05	6.5299E-05	0.0000E+00	0.00	6.61650E-05	0.00000E+00	0.00
	VN06	1.1405E-04	0.0000E+00	0.00	1.15180E-04	0.00000E+00	0.00
	VN07	4.2992E-05	0.0000E+00	0.00	4.22160E-05	0.00000E+00	0.00
	VN08	4.2845E-05	0.0000E+00	0.00	4.21660E-05	0.00000E+00	0.00
	VN09	6.7584E-06	0.0000E+00	0.00	6.65850E-06	0.00000E+00	0.00
	VN10	1.9868E-06	0.0000E+00	0.00	1.83670E-06	0.00000E+00	0.00
	VN11	1.9547E-06	0.0000E+00	0.00	1.79090E-06	0.00000E+00	0.00
	PL01	4.2834E-05	0.0000E+00	0.00	4.17610E-05	0.00000E+00	0.00
	PL02	2.0130E-06	0.0000E+00	0.00	1.92160E-06	0.00000E+00	0.00
	SW01	8.0493E-08	0.0000E+00	0.00			
	SW02	3.5094E-09	0.0000E+00	0.00			
	SW03	0.0000E+00	0.0000E+00	0.00			
	SW04	0.0000E+00	0.0000E+00	0.00			

2.4 Cloud detection

Cloud detection algorithms of GCOM-C algorithms are developed by sharing knowledge of the cloud optical properties mainly studied by the atmosphere group, and implemented in the each algorithm. Simple decision tree will be used for the first version of the land atmospheric correction algorithm.

2.4.1 Decision tree

Following decision tree is applied for solar zenith angle $\theta_0 < 76$ degrees.

if(((rc443<rt443) & (rc868≤0.08) & (sst>-5.0) & (btd<5.0)) & ((elv<1) | ((elv<200) & (vgi<0.1)))) then
 → clear ocean
elseif((rc443<rt443) & (rc868>0.08) & (rc868>1.1×rc443) & (btd<5.0) & (elv>0)) then
 → clear land
elseif((rc443≥0.25) & (rc1640<rc443×rsnow) & (rc1640<rc1050×fsnow) & (rc1380/rs1380<r1380) & (sst<273.15) & (btd<5.0) & (sgr<0.01) & (Ta<278.15)) then
 → clear snow
else
 → cloud
endif

2.4.2 Parameters

- TOA reflectance after gas absorption, rc443, 673, 868, 1050, 1640, 1380 nm
- bright temperature of 11μm band, BT11
- bright temperature of 12μm band, BT12
- bright temperature difference, btd
  btd = BT11−BT12
- air temperature, Ta [K]
- approximate sea surface temperature, sst [K]
  $sst = c_{sst}(1) + c_{sst}(2) \times BT11 + c_{sst}(3) \times btd + c_{sst}(4) \times btd \times pl$
  c_{sst} =(/-1.5258, 1.0054, 2.4108, 0.56367/) ! SST by BT for SGLI (by pstar)
  pl : path length calculated by $1.0/\cos(\theta)-1.0$
  θ : satellite zenith angle
- approximate column water vapor, wvp [mm]
  $wvp = wvc(1) \times btd + wvc(2) \times btd^2$
  wvc =(/11.4821, 5.41933/) ! WV by btd for SGLI (by pstar)
- btd estimated by ancillary column water vapor, bte [K]

dte =btc(1)× wv+btc(2) ×wv^2
btc =(/0.063033,-0.00037827/) ! btd by WV for SGLI (by pstar)

- 1380 nm reflectance without water vapor absorption calculated by interpolation of 1050 nm and 1640 nm, rs1380
rs1380 =(rc1050× (1640−1380)+rc1640× (1380−1050))/(1640−1050)

- threshold of transmittance of 1380nm, r1380
if((|rlat|<snowlat) | ((elv<1500) & (|rlat|<35))) then
r1380=0.95-0.90×epr^2 ! tropical
else
r1380 =1.0 −0.90×epr^2
endif
epr: atmospheric pressure /1013.25 (1.0: 1013.25hPa)
- distribution latitude range of snow areas, snowlat [deg]
snowlat=40 −elv×0.01
elv: land surface elevation [m]
- threshold of 1640nm/1050nm ratio, fsnow
fsnow=0.7
- threshold of 1640nm/443nmratio, rsnow
if(lat<-60) then ! Antarctic
rsnow=0.10
elseif((elv>1000) & (lat> 60) & (lon>-65) & (lon<-20)) then ! GreenLD
rsnow=0.10
elseif(|lat| <snowlat) then ! tropical
rsnow=0.20
elseif((elv<1500) & (|lat| <35)) then ! tropical
rsnow=0.10
else
rsnow=0.28
endif
lat: latitude [deg]
lon: longitude [deg]

- threshold of 443nm reflectance, rt443
if(rc868≤0.08) then
rt443=0.35
else
rt443=0.35–vgi×0.20
if(rt4430<0.16) rt443=0.16
if(rt443>0.35) rt443=0.35
endif

- vegetation index, vgi
vgi=(rc868–rc673)/(rc868+rc673)

2.5 Surface reflectance

2.5.1 Minimum reflectance

Minimum reflectance (a maximum NDVI sample between the 1st and 2nd minimum reflectance samples to avoid shadows) after the molecular reflectance and transmittance (without aerosols), $r_s^{min}(\lambda)$ is used as initial values and index calculations.

2.5.2 Near-UV and blue band reflectance

Near-UV and blue band reflectance, $r_s^{sim}(\lambda)$ is estimated by the NDVI calculated from $r_s^{min}(\lambda)$.

$r_s^{sim}(\lambda)$ is supplementary used for candidate $r_s(\lambda)$ in the multi-temporal variation scheme.

$r_s^{sim}(\lambda)=\max(r_{s1}(\lambda),r_{s2}(\lambda))$

$r_{s1}(\lambda)=a_0(\lambda)+a_1(\lambda)\,NDVI$

$r_{s2}(\lambda)=b_0(\lambda)+b_1(\lambda)\,NDVI$

$LCI = r_s^{min}(868nm) - 1.4989\, r_s^{min}(673nm) + 0.4759\, r_s^{min}(443nm)$

Table 3 Coefficients of surface reflectance estimation by NDVI

λ [nm]	*a0*	*a1*	*b0*	*b1*
380.1	0.2984	-0.9837	0.0355	-0.0272
412.6	0.2951	-0.9297	0.0422	-0.0338
443.3	0.2921	-0.8969	0.0474	-0.0377
489.9	0.2912	-0.8690	0.0546	-0.0445
529.7	0.2938	-0.8528	0.0596	-0.0314
566.2	0.2976	-0.8430	0.0751	-0.0448
672.0	0.3040	-0.8029	0.1256	-0.1237
672.2	0.3041	-0.8030	0.1257	-0.1237
763.1	0.3238	-0.7209	0.0374	0.2256
866.8	0.3319	-0.6151	0.078	0.2182
867.2	0.3318	-0.6141	0.0781	0.2182

2.5.3 Multi-temporal variation scheme

This scheme estimate the surface reflectance Rs(λ) by using the general characteristics of temporal variation of surface reflectance is small and temporal variation of atmosphere is large.

Rs(λ) is searched as minimizing temporal variation of Rs(λ) at multiple λ in about a month by testing aerosol models (M) and optical thickness (τ_a).

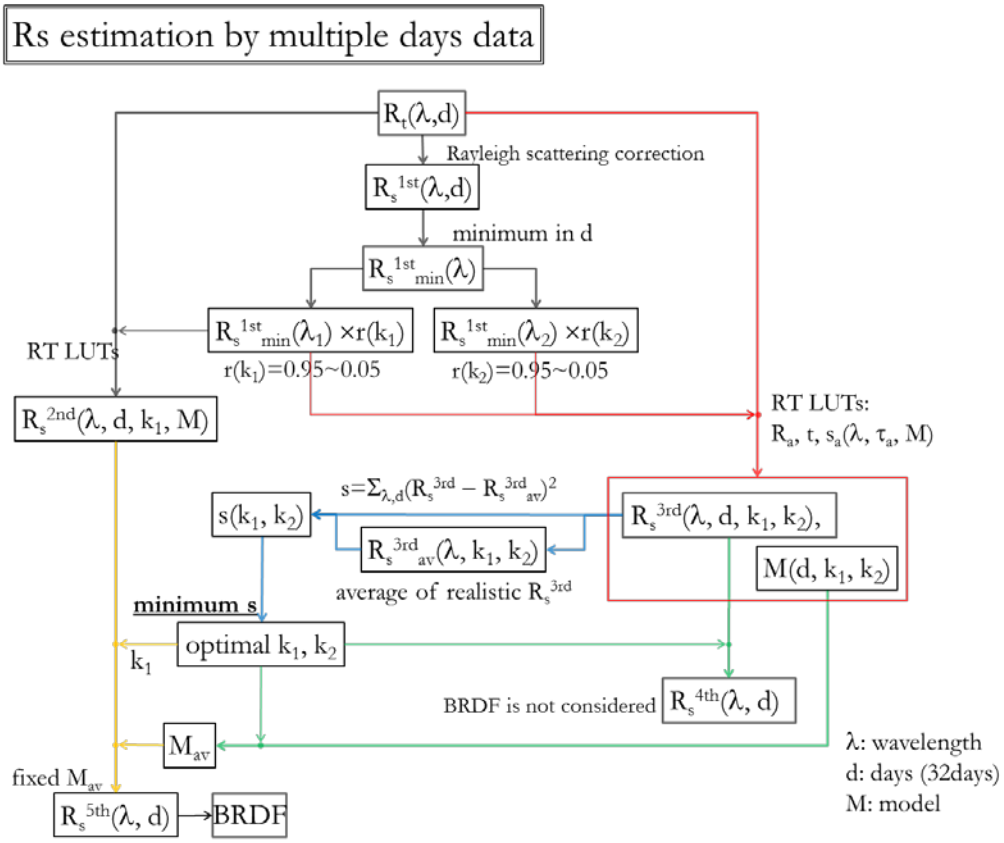

Figure 3 Flow of the multi-temporal variation surface reflectance estimation algorithm

(1) preset several candidate surface reflectance at the base band (λ_{blue}), $Rs(\lambda_{blue})_j$, and estimate τ_a at each M

$$R_t(\lambda) / t' - R_r(\lambda) = R_a(\lambda) + (t_0(\lambda)t_1(\lambda) \times Rs(\lambda)) / (1 - S_a(\lambda) \times Rs(\lambda)) \quad (1)$$

(2) M is calculated by presetting surface reflectance at the reference band $Rs(\lambda_{red})$

(3) surface reflectance at the other bands $Rs(\lambda)_j$ is calculated by the spectral relationship of $R_a(\lambda)$,$t_0(\lambda)t_1(\lambda)$,$S_a(\lambda)$ of the loop-up table

(4) Optimal $Rs(\lambda)$ is selected from the $Rs(\lambda)_j$ (j = 1-32 days) to minimize temporal variation of $Rs(\lambda)$ at multiple bands λ.

(5) BRDF is calculated from $Rs(\lambda)$ calculated by $Rs(\lambda_{blue})$ and mean of M

2.6 Candidate aerosol model

Aerosol models, M, are constructed by mixing the tropospheric and sea-salt particle type aerosols. It is made as look-up tables which include TOA reflectance at solar and satellite geometries, transmittance, aerosol optical thickness, spherical albedo

The aerosol models (particle size distribution, particle shape, and refractive index) will be replaced to the models used in the atmosphere aerosol algorithms in the future.

2.7 Other corrections

2.7.1 Altitude correction

$t_{d0n}=t_{d0}(b,1,1)^{(epr1-1.)}$

$t_{d1n}=t_{d1}(b,1,1)^{(epr1-1.)}$

$r_{rL}(b)= r_{rL}(b) \times Prs$! land

$r_{rO}(b)= r_{rO}(b) \times Prs$! ocean

$s_a(b,t,m)=s_a(b,t,m) \times Prs$

$td0(b,t,m)=td0(b,t,m) \times t_{d0n}$

$td1(b,t,m)=td1(b,t,m) \times t_{d1n}$

2.7.2 molecule scattering correction

$r_{rc}(b) = r_t(b) - r_r(b)$

$r_{s0}(b) = r_{rc}(b) / (t_{d0}(b,1,1) \times t_{d1}(b,1,1) + r_{rc}(b) \times s_a(b,1,1))$

2.7.3 BRF correction

$$\boldsymbol{R(\theta_0, \theta_1, \varphi) = k_0 + k_1 \times F_1(\theta_0, \theta_1, \varphi) + k_2 \times F_2(\theta_0, \theta_1, \varphi)}$$

k_0= *Nadir reflectance*

$$F_1=((\pi - \varphi)\times cos(\varphi)+sin(\varphi)) \times tan(\theta_0) \times tan(\theta_1)/(2 \times \pi) - (tan(\theta_0)+ tan(\theta_1)+ \Delta)/\pi$$

$$F_2=(4/3/\pi)/(cos(\theta_0)+cos(\theta_1)) \times((\pi /2-\alpha) \times cos(\alpha)+sin(\alpha)) \times(1+1/(1+ \alpha /(1.5/180\times\pi))) - 1/3$$

$$\Delta=sqrt(tan(\theta_0)^2+tan(\theta_1)^2 - 2 \times tan(\theta_0) \times tan(\theta_1) \times cos(\varphi))$$

$$\alpha=acos\{cos(\theta_0) \times cos(\theta_1) + sin(\theta_0) \times sin(\theta_1) \times cos(\varphi)\}$$

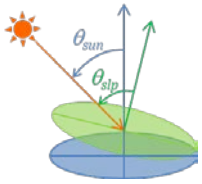

θ_0: *solar zenith,*

θ_1: *satellite zenith,*

φ: *relative azimuth,*

α: *scattering angle*

2.7.4 slope correction (not applied for the at-launch version)

$$R_t/t_g = R_a + (r_{slp}\, t_0\, t_1\, A_s) / (1 - S_a\, A_s)$$

$$A_s = (R_t/t_g - R_a) / (r_{slp}\, t_0\, t_1 + (R_t/t_g - R_a)\, S_a)$$

$$r_{slp} = ((1 - r_{dir})\, cos(\theta_{sun}) + r_{dir}\, cos(\theta_{slp})) / cos(\theta_{sun})$$

$$\theta_{slp} = sin(\theta_{sun})\, cos(\phi_{sun})\, sin(\theta_{slp})\, cos(\phi_{slp}) + sin(\theta_{sun})\, sin(\phi_{sun})\, sin(\theta_{slp})\, sin(\phi_{slp}) + cos(\phi_{sun})\, cos(\phi_{slp})$$

$$r_{dir} = t_b / t_{dif}$$

$$t_b = exp(-(\tau_m + \tau_a))$$

$$t_{dif} = exp(-(\tau_{mb} + (b_{ba0} + b_{ba1}\, \alpha)\, \tau_a))$$

$$\tau_a = \tau_{a0}\, (\lambda/500nm)^{\alpha}$$

2.7.5 center-wavelength correction (not applied for the at-launch version)

The center wavelength is calculated by the center-wavelength shift mode from the ground tests using relative pixel position which is calculated by the pixel address and telescope information （/Geometry_data/Cross_track_section_flag） and satellite zenith angle.

VNR-NPL: $rpix= 9.61898e\text{-}01 - 3.73884e\text{-}02 \times \theta + 3.97139e\text{-}05 \times \theta^2$

VNR-NPN1 : $rpix= -3.73684e\text{-}02 \times \theta - 4.63678e\text{-}05 \times \theta^2$

VNR-NPN2 : $rpix= 3.73684e\text{-}02 \times \theta + 4.63678e\text{-}05 \times \theta^2$

VNR-NPR : $rpix= -9.61898e\text{-}01 + 3.73884e\text{-}02 \times \theta - 3.97139e\text{-}05 \times \theta^2$

VNR-PL1 : $rpix= -8.65696e\text{-}03 \times \theta - 8.81878e\text{-}05 \times \theta^2$

VNR-PL2 : $rpix = 8.65696e\text{-}03 \times \theta + 8.81878e\text{-}05 \times \theta^2$

θ: *satellite zenith angle of VNR-NP (deg)*

$\lambda_c[nm] = c0 + c1*X + c2*X^2 + c3*X^3 + c4*X^4$

X (= -0.5 ~ +0.5): (pixels - center_pixel)/pixel_length

pixels: 1~pixel_length at a telescope

pixel_length=1500 (VNR-NP 250m),

pixel_length=857 (VNR-PL)

c0: center wavelength at the telescope center (X=0)

Molecular scattering table and gas absorption table of minimum and maximum center-wavelength are linear interpolated by the calculated center wavelength.

Table 4 Coefficients of SGLI center wavelength shift

Band	c0	c1	c2	c3	c4	RgErr[nm]	Ave[nm]	Min[nm]	Max[nm]
VNL01	3.7983E+02	-2.0654E-01	4.0953E-01	7.6962E-01	-7.5110E-01	0.005	379.85	379.80	379.91
VNL02	4.1235E+02	1.1515E-01	-7.2607E-02	5.3384E-01	-2.0197E+00	0.005	412.31	412.11	412.38
VNL03	4.4337E+02	9.0581E-02	6.3376E-01	5.5982E-02	7.0385E-02	0.004	443.43	443.37	443.57
VNL04	4.8966E+02	-3.0622E-01	3.3672E-01	4.5020E-01	-3.9824E-01	0.005	489.69	489.60	489.81
VNL05	5.2952E+02	-3.5294E-01	9.6784E-01	-3.1234E-01	1.9387E+00	0.011	529.62	529.47	530.08
VNL06	5.6589E+02	2.4046E-01	8.7851E-01	6.2411E-01	-2.7019E+00	0.008	565.93	565.76	566.12
VNL07	6.7184E+02	-3.4264E-01	7.7027E-01	-6.1871E-01	5.8120E+00	0.020	671.98	671.81	672.61
VNL08	6.7201E+02	-4.1357E-01	6.0967E-01	1.8496E-01	5.3048E+00	0.018	672.13	671.96	672.65
VNL09	7.6327E+02	3.1900E-01	-2.6370E+00	-1.6204E+00	-4.7683E+00	0.008	762.96	762.35	763.28
VNL10	8.6738E+02	1.8538E+00	-1.3750E+01	-1.2301E+01	4.8520E+01	0.046	866.83	866.23	867.48
VNL11	8.6759E+02	1.8948E+00	-1.3941E+01	-1.2742E+01	4.8163E+01	0.042	867.02	866.40	867.70
VNN01	3.8001E+02	1.7104E-01	2.9402E-01	-6.5029E-01	-6.9351E-01	0.005	380.03	379.99	380.08
VNN02	4.1257E+02	1.6869E-01	-2.2033E-01	4.3098E-01	-1.9828E+00	0.008	412.52	412.28	412.60
VNN03	4.4316E+02	-9.9156E-02	7.1108E-01	-1.6487E-02	4.1156E-01	0.005	443.23	443.16	443.40
VNN04	4.8983E+02	2.8187E-01	2.9698E-01	-3.6911E-01	-5.8977E-01	0.005	489.85	489.77	489.97
VNN05	5.2952E+02	3.9348E-01	8.8587E-01	2.7552E-01	2.0914E+00	0.010	529.63	529.48	530.09
VNN06	5.6613E+02	2.9743E-01	7.9222E-01	4.1063E-01	-2.9697E+00	0.007	566.16	565.96	566.34
VNN07	6.7182E+02	3.8590E-01	1.2226E+00	-2.3696E-02	3.8871E+00	0.022	671.97	671.76	672.55
VNN08	6.7194E+02	4.3907E-01	7.5132E-01	2.2127E-02	5.3565E+00	0.018	672.08	671.89	672.66
VNN09	7.6342E+02	-3.1793E-01	-2.5845E+00	1.6389E+00	-4.8441E+00	0.008	763.12	762.51	763.43
VNN10	8.6730E+02	-1.7540E+00	-1.3713E+01	1.2056E+01	4.8410E+01	0.045	866.76	866.18	867.43
VNN11	8.6767E+02	-1.8758E+00	-1.3568E+01	1.2824E+01	4.7018E+01	0.032	867.12	866.50	867.81
VNR01	3.8020E+02	-1.4418E-01	2.5644E-01	6.5340E-01	-9.4438E-01	0.006	380.21	380.18	380.24
VNR02	4.1265E+02	2.0817E-01	-3.2323E-01	3.4006E-01	-1.7034E+00	0.006	412.60	412.34	412.68
VNR03	4.4296E+02	1.0681E-01	8.1284E-01	-3.6629E-02	7.1595E-01	0.004	443.04	442.96	443.24
VNR04	4.9032E+02	-2.2237E-01	1.0639E-02	2.1432E-01	-5.0950E-01	0.007	490.31	490.21	490.39
VNR05	5.2955E+02	-4.1437E-01	9.1150E-01	-1.2109E-01	1.6420E+00	0.011	529.65	529.50	530.09
VNR06	5.6636E+02	3.4432E-01	7.4963E-01	2.2421E-01	-3.3094E+00	0.006	566.38	566.16	566.56
VNR07	6.7177E+02	-4.0534E-01	1.1152E+00	-1.8236E-01	4.7486E+00	0.018	671.93	671.73	672.55
VNR08	6.7198E+02	-5.0520E-01	6.5910E-01	2.4386E-01	5.1359E+00	0.017	672.10	671.91	672.67
VNR09	7.6357E+02	3.0504E-01	-2.5451E+00	-1.5900E+00	-4.8479E+00	0.007	763.28	762.68	763.58
VNR10	8.6725E+02	1.7793E+00	-1.3803E+01	-1.2226E+01	4.9354E+01	0.048	866.71	866.11	867.44
VNR11	8.6760E+02	2.0163E+00	-1.3424E+01	-1.4051E+01	4.8480E+01	0.034	867.08	866.46	867.90
VNP01	6.7191e+02	-3.3244e-01	1.2376e+01	1.2811e+00	-3.2838e+01	0.023	672.54	671.89	673.10
VNP02	8.6620e+02	-1.7438e+00	1.0498e+00	5.1759e+00	-5.6396e+00	0.007	866.22	865.85	866.63

Coefficients c0~c4, regression error, Average, Min and Max of center wavelengths of VNL (VNR-NP telescope -Left), VNN (VNR-NP telescope-Nadir), VNR (VNR-NP telescope-Right) and VNR-PL. The coefficients were calculated by EORC using original measurements by SGLI sensor team)

2.8 Mask/Flag

The first 0-1bits are common for the Level-2 products, input data lack and land/water flags. Others are defined as the right table. Cloud masks are set by the target date, and the probably cloud is set by the multiple day tests (they can be changed post launch). The Level-3 statistics processing will use data with the QAflag of bit4, 6, and 8=0 and the product value is within the valid range. Bit13-15 will be used to indicate the error level of the product.

Table 5 Bit specification of QA_flag

bit	Description	Level-3 mask
0	no data (mask)	0
1	Land (0: ocean, 1: land)	0
2	coast (flag)	0
3	sunglint flag	0
4	sunglint mask	1
5	snow or ice (flag)	0
6	cloud (mask)	1
7	probably cloud (by multi-day)	0
8	high tau-a (flag)	1
9	no BRF(mask)	0
10	BRF samples<=3	0
11	stray light	0
12	shadow (mask)	0
13	quality level TBD	0
14	quality level TBD	0
15	quality level TBD	0

3 Validation plan

3.1 Error budget estimation

3.1.1 TBD

3.2 Validation method after launch

3.2.1 Data release threshold accuracy：0.3 (≤443nm), 0.2 (>443nm) *

It is calculated as root mean square (RMS) difference (RMSD) between the instantaneous satellite estimates and in-situ measurements where AOT at 500nm less than 0.25

3.2.2 Standard accuracy：0.1 (≤443nm), 0.05 (>443nm) *

Same as the above

3.2.3 Target accuracy: 0.05 (≤443nm), 0.025 (>443nm) *

Same as the above

note: Defined with land reflectance~0.2, solar zenith<30deg, and flat surface

3.2.4 acquisition of validation data

In-situ data will be obtained mainly by the GCOM-C PIs at Yatsugatake, JAXA super site 500, JaLTER, JapanFlux, PEN sites and so on.

- Honda of Chiba Univ.（Spectral reflectance (incl. BRDF) data measured by FieldSpec, MS-720、Hyperspectral Camera from UAV、Spectral data measured from UAV. BiRS simulations will be used for uniform surfaces）、

- Nasahara of Tsukuba Univ.（Spectral data measured by MS-720 and MS-700 from Tower）

3.2.5 Comparison with MODIS BRDF product

Validation of special distribution and stability of the retrievals

4 Remaining issues

4.1 SGLI calibration sensitivities

- center-wavelength correction
- polarization sensitivity correction (applied after post-launch evaluation, especially for 380nm)

4.2 Product validation

- comparison with in-situ data
- comparison with the MODIS BRDF product

4.3 Validation of slope correction

Decision of application after evaluation of the improvement by the correction

4.4 Cloud detection evaluation and improvement

Validation and optimization of the cloud detection

4.5 Use of LAI BRF model

It will be investigated after validation of the LAI model

4.6 Use of multi-angle and polarization

It will be investigated after launch with consistency with the downstream algorithms

4.7 Adjacent effect

The efficiency will be investigated after launch

4.8 Consistency evaluation with atmosphere algorithms (RSRF is used as boundary condition) and numerical models

It will be investigated after launch

References

F. Maignan, F.-M. Breon, R. Lacaze, Bidirectional reflectance of Earth targets: Evaluation of analytical models using a large set of spaceborne measurements with emphasis on the Hot Spot, Remote Sensing of Environment 90 (2004) 210–220.

Alexei I. Lyapustin, Yujie Wang, Istvan Laszlo, Thomas Hilker, Forrest G.Hall, Piers J. Sellers, Compton J. Tucker , Sergey V. Korkin: Multi-angle implementation of atmospheric correction for MODIS (MAIAC): 3. Atmospheric correction , Remote Sensing of Environment 127 (2012) 385–393.

Mahmoud El Hajj, Agnès Bégué, Bruno Lafrance, Olivier Hagolle, Gérard Dedieu and Matthieu Rumeau, Relative Radiometric Normalization and Atmospheric Correction of a SPOT 5 Time Series, Sensors 2008, 8, 2774-2791.

Olivier Hagolle, Gérard Dedieu, Bernard Mougenot, Vincent Debaecker, Benoit Duchemin, et al.. Correction of aerosol effects on multi-temporal images acquired with constant viewing angles: application to Formosat-2 images. Remote Sensing of Environment, Elsevier, 2008, 112(4), pp.1689-1701.